

Compositional grading of $\text{In}_x\text{Ga}_{1-x}\text{As}/\text{GaAs}$ tunnel junctions enhanced by ErAs nanoparticles

R. Salas*, E. M. Krivoy, A. M. Crook, H. P. Nair, and S. R. Bank
Microelectronics Research Center, University of Texas, Austin, TX 78758;

ABSTRACT

We investigate the electrical conductivity of GaAs-based tunnel junctions enhanced with semimetallic ErAs nanoparticles. In particular, we examine the effects of digitally-graded InGaAs alloys on the n-type side of the tunnel junction, along with different p-type doping levels. Device characteristics of the graded structures indicate that the n-type Schottky barrier may not be the limiting factor in the tunneling current as initially hypothesized. Moreover, significantly improved forward and reverse bias tunneling currents were observed with increased p-type doping, suggesting p-side limitation.

Keywords: ErAs, GaAs, InGaAs, Tunnel junction, Compositional grading

1. INTRODUCTION

Low-resistivity tunnel junctions enhance the performance of many photonic devices. Tunnel junctions can be used as interconnects between n- and p-doped layers of different band gap junctions in multijunction solar cells.^{1,2} Vertical-cavity surface-emitting lasers (VCSELs) are another example where tunnel junctions play an important role in device performance, enabling the electrically and optically lossy p-type Distributed Bragg Reflectors (DBRs) to be replaced with an n-type DBR.^{4,5} Tunnel junctions also find application in nipnip photomixers for THz generation, where the pn junctions are subjected to high current densities and must drop very little voltage.³ Conventional tunnel junctions consist of heavily doped p^+/n^+ regions (Figure 1a) where band-to-band tunneling through the depletion region is the dominant current flow mechanism.⁶ To first order, the tunneling current is exponentially dependent on the depletion width (barrier height) and bandgap (barrier length) of the junction.⁷

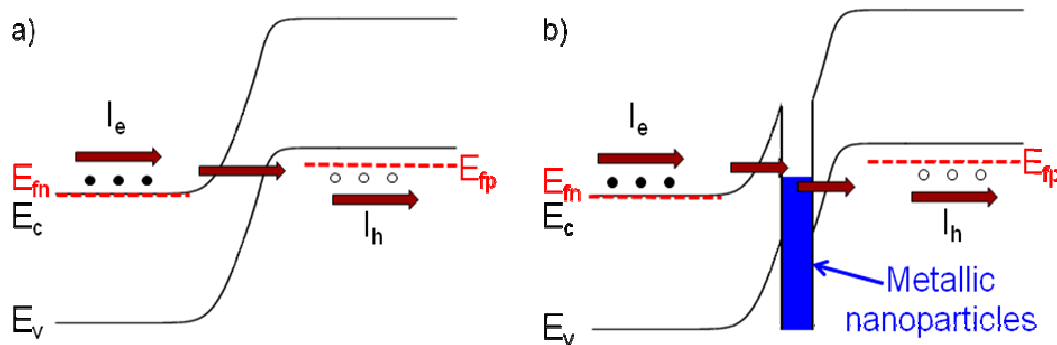


Figure 1. Band diagram of (a) a conventional tunnel junction and (b) an ErAs nanoparticle-enhanced tunnel junction.

Introducing states within the bandgap of the tunnel junction, through the incorporation of excess arsenic during low-temperature growth, has significantly enhanced the conductivity of GaAs tunnel junctions.^{8,9} Since the tunneling probability is dependent on the barrier height and length, introducing trapped states in the gap splits the tunneling mechanism into two smaller steps.⁹ Although the tunneling current has been shown to improve by many orders of magnitude, the improvement is dependent on the limited density of states, which require phonon assisted tunneling, and

the thermal robustness of the arsenic trapped levels.⁸ By contrast, introducing semimetallic nanoparticles of ErAs⁹ introduces a continuum of states in energy, as well as significantly improving thermal stability. As shown in Figure 1b, the ErAs nanoparticles transform the tunnel junction into essentially two back-to-back Schottky contacts. Previous work with ErAs films on GaAs¹⁰ has shown that the Fermi level in the ErAs layer is ~ 0.85 eV below the conduction band of GaAs, which places it approximately in the middle of the gap. However, further work with ErAs in InGaAs and AlGaAs has also shown that the Schottky barrier height is tunable through compositional grading, doping, and interface type.^{11,12} Although high quality ErAs films on GaAs have been demonstrated, the GaAs overgrowth suffered from a high density of antiphase domains.¹³ Growing ErAs self-assembled nanoparticles instead of full films, however, has shown high quality GaAs overgrowth by seeding through the exposed GaAs¹⁴ making it ideal for optical applications.⁹ The ErAs nanostructure morphology provides an additional route to improving tunneling currents, which is tunable through the growth temperature and amount of ErAs deposited.¹⁵

In this study, we seek to explore the ultimate limits of the conductivity through the ErAs nanoparticle-enhanced tunnel junction via band engineering. Since the Fermi level of ErAs films align closer to the valence band edge than the conduction band edge, it was expected that tunneling currents would be limited by the n-type Schottky contact in tunnel junctions with nanoparticles. Consequently, we investigated the effect of digitally grading the n-type side of the tunnel junction from GaAs to $\text{In}_{0.5}\text{Ga}_{0.5}\text{As}$, as a mechanism for lowering the n-type Schottky barrier. However, measured I-V characteristics of the graded and ungraded tunnel junctions showed no improvement in the conductivity, possibly pointing to a p-type Schottky contact limitation. Therefore, we also investigated the graded and ungraded ErAs tunnel junctions with higher p-type doping to uncover the dominant limiting Schottky contact.

2. EXPERIMENTAL RESULTS AND DISCUSSION

Samples were grown on n-type $1\text{-}5 \times 10^{18} \text{ cm}^{-3}$ silicon-doped (100) GaAs wafers by solid-source molecular beam epitaxy (MBE), in a Varian Gen II system. The semiconductor and ErAs layers were grown at 530°C , as measured by a pyrometer calibrated to the GaAs surface oxide desorption temperature. The beam equivalent pressure (BEP) ratios were 20 for GaAs (As_2/Ga) and 121 (As_2/Er) for ErAs. The device structures investigated are shown in Table I: (1) a conventional tunnel junction with $n_{\text{Si}}=5 \times 10^{18} \text{ cm}^{-3}$ and $p_{\text{Be}}=10^{19} \text{ cm}^{-3}$; (2) a digitally graded GaAs to $\text{In}_{0.5}\text{Ga}_{0.5}\text{As}$ in five steps with $n_{\text{Si}}=5 \times 10^{18} \text{ cm}^{-3}$ and $p_{\text{Be}}=10^{19} \text{ cm}^{-3}$; (3) a tunnel junction with 1.33 monolayers (ML) of ErAs placed at the interface of the junction with $n_{\text{Si}}=5 \times 10^{18} \text{ cm}^{-3}$ and $p_{\text{Be}}=10^{19} \text{ cm}^{-3}$; (4) a digitally graded GaAs to $\text{In}_{0.5}\text{Ga}_{0.5}\text{As}$ in five steps with 1.33 ML of ErAs placed at the interface with $n_{\text{Si}}=5 \times 10^{18} \text{ cm}^{-3}$ and $p_{\text{Be}}=10^{19} \text{ cm}^{-3}$; (5) a tunnel junction with 1.33 ML of ErAs placed at the interface with $n_{\text{Si}}=5 \times 10^{18} \text{ cm}^{-3}$ and $p_{\text{Be}}=5 \times 10^{19} \text{ cm}^{-3}$; (6) a digitally graded GaAs to $\text{In}_{0.5}\text{Ga}_{0.5}\text{As}$ in five steps with 1.33 ML of ErAs placed at the interface with $n_{\text{Si}}=5 \times 10^{18} \text{ cm}^{-3}$ and $p_{\text{Be}}=5 \times 10^{19} \text{ cm}^{-3}$.

Samples were processed into circular mesas with radii ranging from $15 \mu\text{m}$ to $100 \mu\text{m}$ with electron beam evaporation of Ti/Au for the top contacts and Au/Ge/Ni/Au for the bottom contacts, followed by a self-aligned inductively coupled plasma dry etch with SiCl_4 and Ar. Profilometer measurements of the etched mesa structures yielded an average etch of $\sim 400 \text{ nm}$, well below the tunneling interface where the ErAs nanoparticles are located.

Since n-dopant species such as silicon become amphoteric at high concentrations in GaAs,⁸ the active electron concentration is limited to $5 \times 10^8 \text{ cm}^{-3}$. The higher n-side Schottky barrier (~ 0.8 eV barrier height), coupled with the limited n-type doping, led us to assume the n-type side was limiting conductivity. Figure 2 shows the band diagrams of each structure calculated with a 1-D Poisson solver that accounts for strain effects, under the assumption that the ErAs nanoparticles had the same work function as ErAs films grown on GaAs. The resulting Schottky barrier height of the ErAs/InGaAs graded device was calculated to be ~ 0.2 eV lower than the ErAs/GaAs device. Consequently, we expected the conductivity to improve with the InGaAs grading on the n-type side of the tunnel junction. However, the measured I-V characteristics for devices 1-4, shown in Figure 3, are approximately the same for Device 4 (ErAs/InGaAs graded) and Device 3 (ErAs/GaAs) tunnel junctions, under both forward and reverse bias. This is somewhat surprising as ErAs-free devices showed the opposite trend. These results contradict the initial hypothesis that the nanoparticle enhanced tunnel junctions are limited by the n-type side Schottky barrier.

Table I. Investigated devices.

	Layer Structure (Doping Type [Species] Material)	Active Doping Concentration (cm^{-3})	Layer Thicknesses (nm)
1) GaAs Conventional Tunnel Junction	p^+ [Be] GaAs n^+ [Si] GaAs n^+ [Si] Substrate GaAs	1×10^{19} 5×10^{18} $1-5 \times 10^{18}$	200 200 $625 \mu\text{m}$
2) InGaAs Graded Tunnel Junction	p^+ [Be] GaAs n^+ [Si] $\text{In}_x\text{Ga}_{1-x}\text{As}$ (5 steps to $x=0.5$) n^+ [Si] GaAs n^+ [Si] Substrate GaAs	1×10^{19} 5×10^{18} 5×10^{18} $1-5 \times 10^{18}$	200 10 200 $625 \mu\text{m}$
3) ErAs/GaAs Tunnel Junction	p^+ [Be] GaAs ErAs n^+ [Si] GaAs n^+ [Si] Substrate GaAs	1×10^{19} 5×10^{18} $1-5 \times 10^{18}$	200 0.76 nm (1.33 ML) 200 $625 \mu\text{m}$
4) ErAs/InGaAs Graded Tunnel Junction	p^+ [Be] GaAs ErAs n^+ [Si] $\text{In}_x\text{Ga}_{1-x}\text{As}$ (5 steps to $x=0.5$) n^+ [Si] GaAs n^+ [Si] Substrate GaAs	1×10^{19} 5×10^{18} 5×10^{18} $1-5 \times 10^{18}$	200 0.76 nm (1.33 ML) 10 200 $625 \mu\text{m}$
5) ErAs/GaAs Tunnel Junction	p^+ [Be] GaAs ErAs n^+ [Si] GaAs n^+ [Si] Substrate GaAs	5×10^{19} 5×10^{18} $1-5 \times 10^{18}$	200 0.76 nm (1.33 ML) 200 $625 \mu\text{m}$
6) ErAs/InGaAs Graded Tunnel Junction	p^+ [Be] GaAs ErAs n^+ [Si] $\text{In}_x\text{Ga}_{1-x}\text{As}$ (5 steps to $x=0.5$) n^+ [Si] GaAs n^+ [Si] Substrate GaAs	5×10^{19} 5×10^{18} 5×10^{18} $1-5 \times 10^{18}$	200 0.76 nm (1.33 ML) 10 200 $625 \mu\text{m}$

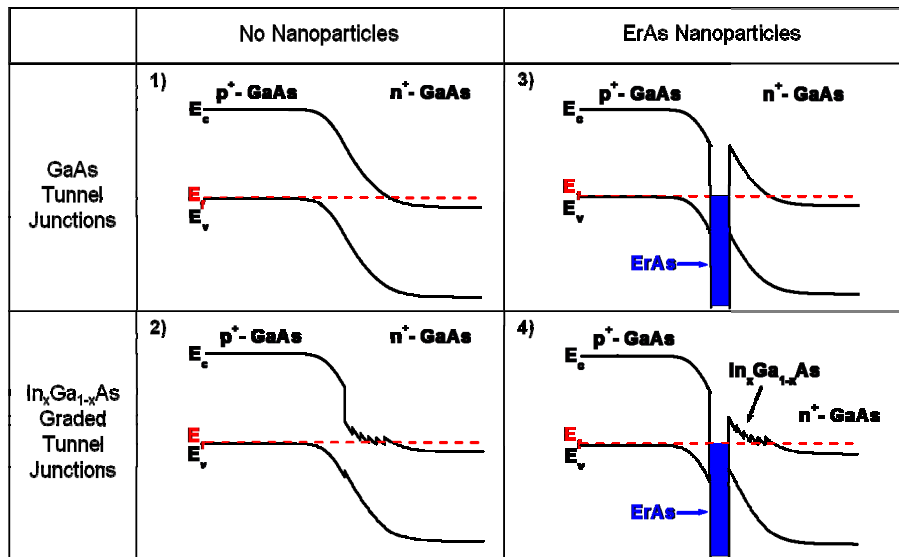


Figure 2. Band diagram of investigated devices 1-4 with beryllium concentration of 10^{19} cm^{-3} . Band models are simulated with a 1-D Poisson that accounts for strain effects.

Based on the lack of improvement in the conductivity of Device 4 compared to Device 3 shown in Figure 3, we increased the p-doping and examined its effect on the conductivity. Figure 4, shows that higher p-type doping in Device 5 increased the measured current density by an order of magnitude at 0.5 V of forward bias and moderately in reverse bias over Device 3. Device 6 with high p-doping, however, worsened significantly compared to Device 4 at the lower doping. We now speculate that the limiting side is perhaps the p-type Schottky barrier and by increasing the doping concentration, we decrease the length of the barrier on the p-type side. Since we are using beryllium as the p-dopant, we attribute the degradation in conductivity of Device 6 to diffusion of beryllium, which has been shown to trend higher under an InAs molar fraction of greater than 0.07 on GaAs.¹⁶ We suspect that the beryllium may have diffused into the n-type InGaAs, shifting the pn interface towards the n-side and away from the nanoparticles. The band structure would then become a conventional tunnel junction followed by two back-to-back p-type Schottky barriers that in turn would add significant series resistance to the device, consistent with the device results.

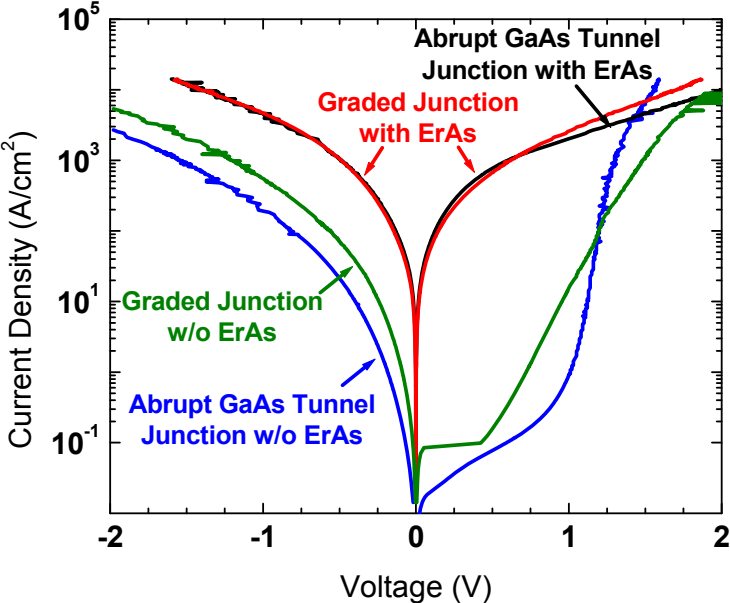


Figure 3. Tunnel junction current density vs. voltage. Note that the graded ErAs tunnel junction has almost the same conductivity as the GaAs/ErAs tunnel junction.

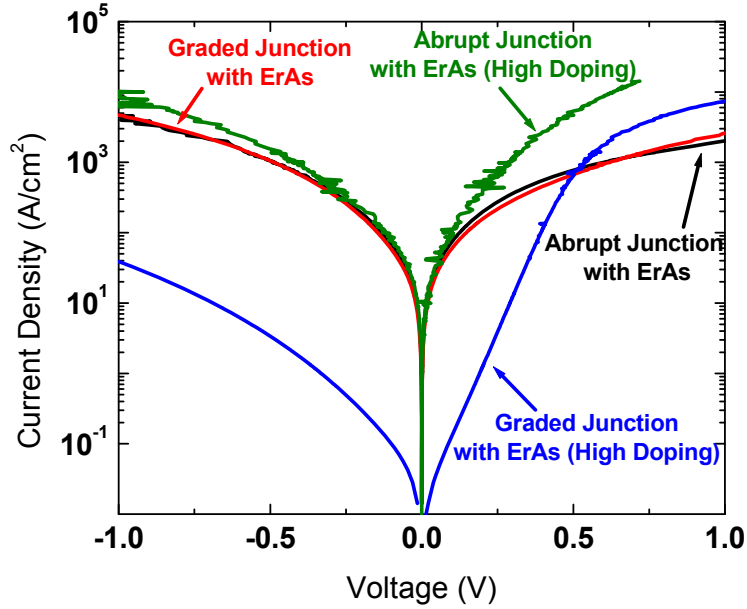


Figure 4. Tunnel junction current density vs. voltage for graded and ungraded devices with high ($5 \times 10^{19} \text{ cm}^{-3}$) and low (10^{19} cm^{-3}) p-type doping.

3. CONCLUSIONS

We have investigated the electrical characteristics of tunnel junctions enhanced with ErAs nanoparticles, with the aim of finding the ultimate limits of the conductivity by engineering the band gap on the n-type side and varying the doping levels on the p-type side. Current densities of 5 kA/cm^2 at 0.5 V were measured under forward bias for the high p-doped ($5 \times 10^{19} \text{ cm}^{-3}$) ungraded ErAs tunnel junction. We found that the conductivity limitations were dominated by the p-type Schottky barrier, since no significant improvement was measured by lowering the n-type barrier. Furthermore, the high p-doped InGaAs tunnel junction was degraded significantly, in comparison to the more lightly-doped device. We attribute this degradation to beryllium diffusion.

References

- [1] Zide J M O, Kleiman-Shwarscstein A, Strandwitz N C, Zimmerman J D, Steenblock-Smith A, Gossard A C, Forman A, Ivanovskaya A and Stucky G D, "Increased efficiency in multijunction solar cells through the incorporation of semimetallic ErAs nanoparticles into the tunnel junction," *Appl. Phys. Lett.* **88**, 162103 (2006).
- [2] Cotal H, Fetzer C, Boisvert J, Kinsey G, King R, Hebert P, Yoon H, Karam N, "III-V multijunction solar cells for concentrating photovoltaics," *Energy Environ. Sci.* **2**, 174 (2009).
- [3] Preu S, Renner F H, Malzer S, Dohler G H, Wang L J, Wilkinson T L J, Brown E R, Hanson M and Gossard A C "Efficient terahertz emission from ballistic transport-enhanced n-i-p-n-i-p superlattice photomixers," *Appl. Phys. Lett.* **90**, 212115 (2007).
- [4] Mehta M, Feezell D, Buell D A, Jackson A W, Coldren L A and Bowers J E 2006 "Electrical design optimization of single-mode tunnel-junction-based long-wavelength VCSELs," *IEEE J. Quantum Electron.* **42**, 675.
- [5] Ortsiefer M, Shau R, Bohm G and Amann M-C 2000 "Low-threshold index-guided 1.5 μm long-wavelength vertical-cavity surface-emitting laser with high efficiency," *Appl. Phys. Lett.* **76**, 2179.
- [6] Esaki L, "New phenomenon in narrow germanium p-n junctions," *Phys. Rev.* **109**, 603-604 (1958).
- [7] Preu S, Malzer S, Dohler G H, Lu H, Gossard A C, and Wang L J, "Efficient III-V tunneling diodes with ErAs recombination centers," *Semicond. Sci. Technol.* **25**, 115004 (2010).
- [8] Ahmed S, Melloch M R, Harmon E S, McInturff D T, Woodall J M, "Use of nonstoichiometry to form GaAs tunnel junctions," *Appl. Phys. Lett.* **71**, 3667 (1997).
- [9] Pohl P, Renner F H, Eckardt M, Schwahauber A, Friedrich A, Yuksekdog O, Malzer S, Dohler G H, "Enhanced recombination tunneling in GaAs pn junctions containing low temperature-grow GaAs and ErAs layers," *Appl. Phys. Lett.* **83**, 19-4035 (2003).
- [10] Palmstrom C J, Cheeks T L, Gilchrist H L, Zhu J G, Carter C B, Wilkens B J, Martin R, "Effect of orientation on the Schottky barrier height of thermodynamically stable epitaxial metal/GaAs structures," *J. Vac. Sci. Technol.* **A10**, 4 (1992).
- [11] Driscoll D C, Hanson M, Kadow C, Gossard A C, "Electronic structure and conduction in a metal-semiconductor digital composite: ErAs:InGaAs," *Appl. Phys. Lett.* **78**, 121703 (2001).
- [12] Zimmerman J D, Brown E R, Gossard A C, "Tunable all epitaxial semimetal-semiconductor Schottky diode system: ErAs on InAlGaAs," *J. Vac. Sci. Technol. B* **23**, 5 (2005).
- [13] Palmstrom C J, Garison K C, Mounier S, Sands T, Schwartz C L, Tabatabaie N, Allen S J, Gilchrist H L, Miceli P F, "Growth of epitaxial rare-earth arsenide/(100) GaAs and GaAs/rare-earth arsenide/(100)GaAs structures," *J. Vac. Sci. Technol. B* **7**, 747 (1989).
- [14] Kadow C, Fleischer S B, Ibbertson J P, Bowers J E, Gossard A C, Dong J W, Palmstrom C J, "Self assembled ErAs islands in GaAs: Growth and subpicosecond carrier dynamics," *Appl. Phys. Lett.* **75**, 3548 (1999).
- [15] Nair H P, Crook A C, Bank S R, "Enhanced conductivity of tunnel junctions employing semimetallic nanoparticles through variation in growth temperature and deposition," *Appl. Phys. Lett.* **96**, 222104 (2010).
- [16] Tomioka T, Fujii T, Ishikawa H, Sasa S, Endoh A, Bamba Y, Ishii K, Kataoka Y, "Suppression of beryllium diffusion by incorporating indium in AlGaAs for HBT applications using molecular beam epitaxy," *Jnp. J. Appl. Phys. Lett.* **29**, L716 (1990).